Effect of temperature and phase transition on oxidation resistance of low density lipoprotein

Pilar Ramos,* Steven Paul Gieseg,* Bernhard Schuster,† and Hermann Esterbauer[1,*]

Institute of Biochemistry,* University of Graz, A-8010 Graz, Austria, and Institute of Biophysics and X-ray Structure Research,† Austrian Academy of Sciences, A-8010 Graz, Austria

Abstract The study of the effect of temperature on the kinetics of low density lipoprotein (LDL) oxidation was carried out by measuring the conjugated diene (CD) versus time curves at a fixed LDL concentration (0.1 μM) and at different Cu^{2+} concentrations (0.5–10 μM) in a wide temperature range, from 10°C to 45°C. The core melting point of the LDL determined with differential scanning calorimetry was 31.1°C. We have demonstrated that temperature exerts a clear effect in the Cu^{2+}-meditated LDL oxidation, with a strong decrease in lag time and a notable increase in the rate of propagation. This temperature dependence of lag time and rate of propagation fully obeys the Arrhenius law, suggesting that the core melting point of the LDL has no or only a minor effect on these oxidation indices. The Arrhenius plots of the binding of Cu^{2+} to LDL, measured by K, gave two breaks suggesting that this value is affected by the core transition of the LDL as well as by structural changes at around 15°C. The mean activation energy during rate of initiation was 13.5 kcal/mol and tended to decrease with increasing Cu^{2+} concentration. The activation energy in the propagation phase was 10.6 kcal/mol and was independent of Cu^{2+} concentration. In this work we have also shown that the CD method can be conducted with high reproducibility and that a sucrose-supplemented plasma frozen at -80°C can be used as a source of LDL with an unvarying vitamin E content and reproducible oxidation properties.—**Ramos, P., S. P. Gieseg, B. Schuster, and H. Esterbauer.** Effect of temperature and phase transition on oxidation resistance of low density lipoprotein. *J. Lipid Res.* 1995. **36:** 2113–2128.

Supplementary key words copper oxidation kinetics • temperature • conjugated dienes • lag phase • copper binding sites • activation energy • LDL storage

There is increasing evidence that oxidatively modified low density lipoprotein (LDL) is an important mediator in the pathogenesis of atherosclerosis (1–3). Oxidation of LDL is a rather complex process during which chemical, structural, and functional properties of the LDL lipids and apolipoprotein B (apoB) progressively change (2, 4, 5).

The conjugated diene method (CD method) has become one of the most frequently used assays to assess oxidation resistance of LDL. In the CD method (6), copper is added as prooxidant to an LDL solution, and the lipid peroxidation process is then followed by recording the increase of the UV-absorption at 234 nm. With this method, several oxidation indices can be determined such as lag time, rate of oxidation, or the maximum amount of formed dienes. The oxidation resistance of LDL depends on intrinsic properties of the lipoprotein and on the experimental conditions (2, 7).

One variable that can strongly affect the kinetics of LDL oxidation is temperature (8–10). Temperature should have a dual effect. First, rate of oxidation should increase, as predicted by temperature dependence of chemical reactions, and second, the process may significantly change depending on whether oxidation occurs above or below the transition temperature of LDL. It is known that the core lipids of LDL may occur in a rigid or fluid state (11, 12). The temperature of the phase-transition (T_m) is one of the parameters obtained by DSC experiments and is, by definition, the midpoint temperature of the transition where the lipids coexist in an equilibrium state. LDL undergoes two thermal transitions (11, 12). The first one, associated with the reversible order–disorder transition of the core located cholesteryl esters, is reversible and takes place over the range 20–40°C depending on triglyceride content (11, 13, 14). The second transition, associated with the disruption of the LDL particle and protein unfolding and denaturation, is irreversible and occurs over the temperature range of 70–90°C (15, 16). Recently, it was

Abbreviations: apoB, apolipoprotein B; BHT, butylated hydroxytoluene; CD, conjugated dienes; DSC, differential scanning calorimetry; E_a, activation energy; EDTA, ethylenediamine tetraacetic acid disodium salt; LDL, low density lipoprotein; PBS, phosphate-buffered saline; t_1, lag time; t_2, oxidation time required for half maximal dienes; T_m, midpoint temperature of the phase transition; t_1*, minimum value of lag time at infinite copper concentration; v, propagation rate; v*, propagation rate at infinite copper concentration.

[1]To whom correspondence should be addressed.

shown that oxidation of dense LDL subfractions with 10 μM Cu^{2+}, as measured by lag time and propagation rate, is affected by core transition (10). The present study was designed to determine, using an LDL pool and the CD method, the influence of temperature and copper concentration on LDL oxidation and to assess whether the lipid phase transition affects the activation enegy, Cu^{2+} binding properties, and oxidation resistance of LDL.

MATERIAL AND METHODS

Reagents

The reagents used were of AR grade or better, obtained from Merck (Germany) or Sigma (St. Louis, MO). All solutions were prepared from ion-exchanged laboratory water filtered through a Millipore Norganic cartridge (Millipore Corporation, MA).

Storage of plasma and preparation of LDL

EDTA-containing plasma samples (1 mg EDTA/mL) were prepared on one day from blood of nine fasted normolipidemic volunteers (age 25–35 years). The plasma samples were pooled, sucrose was added to give a final concentration 0.6%, and then the pool was divided into portions of 12 or 24 mL. One of these portions was used on the same day to prepare LDL and the rest was stored at -80°C for a maximum of 8 weeks. All measurements described in this study were done with LDL prepared from aliquots of this plasma pool. (For effect of storage time on oxidation behavior of LDL, see Table 2).

LDL was prepared by ultracentrifugation using a single-step discontinuous gradient in a Beckman NTV65 rotor at 60,000 rpm for 2 h at 10°C (7). An aliquot of the LDL stock solution was used on the same day for oxidation experiments and the remaining part of the LDL stock solution was filtered through a 0.45-μm filter adapted to a syringe into a sterile, evacuated glass vial (Techne Vial, Mallinckrodt-Diagnostica) and stored under argon gas in the dark at 4°C up to 2 weeks.

Vitamin E analysis

α- and γ-tocopherol content in LDL (17) was determined from aliquots of the lipid extracts as described earlier (18). Briefly, a sample of 0.5 mg mass LDL in 0.5 mL bidistilled water (containing 1 mg/mL EDTA and 0.5 mg/mL BHT) was mixed with 0.5 mL of iced ethanol. Then 1 mL of n-hexane was added and after centrifugation 0.8 mL of the hexane phase was dried under nitrogen. The residue was dissolved in acetonitrile and analyzed by HPLC on a Merck Lichrocart 125-4, Lichrospher 100 RP-18 (5 μm) column, with 95% methanol as mobile phase (1 mL/min) and a fluorescence detector set at an excitation of 292 nm and an emission of 335 nm.

LDL oxidation

Before oxidation, a volume of 0.5–0.9 mL of the LDL stock solution was desalted and made EDTA free by gel-filtration in Econo-Pac 10DG columns (Bio-Rad, Richmond, CA) with PBS (10 mM sodium phosphate buffer, pH 7.4, containing 0.15 M sodium chloride) as eluting buffer (8). To remove contaminating transition metal ions, the PBS solution was previously stirred with 5 g/L of Chelex-100 resin (Bio-Rad). The LDL concentration in the PBS solution was then determined by measuring total cholesterol with the CHOD-PAP enzymatic test kit (Boehringer-Mannheim, Germany). The LDL concentration is expressed as μM, assuming an LDL molecular weight of 2.5 MDa and a cholesterol content of 31.6 weight %.

The LDL oxidation process was followed by recording the conjugated diene absorption at 234 nm in a Beckman DU-640 spectrometer. The instrument was equipped with an auto-cell holder for six cuvettes (this allowed us to measure CD curves for six samples simultaneously) and the temperature was kept constant by a Peltier element. Appropriate volumes of the EDTA-free LDL solutions and PBS (kept in a water bath at the desired temperature) were pipetted into the set of six quartz cuvettes and the oxidation process was started by adding freshly prepared aqueous solutions of $CuSO_4$. The final concentration of LDL was, in all experiments, 0.1 μM (equal to 50 μg protein/mL or 0.25 mg LDL mass/mL). The final concentrations of $CuSO_4$ were 0.5, 0.7, 1.0, 1.6, and 5.0 μM for the temperature range of 20°C to 45°C; for 10°C, and 15°C the $CuSO_4$ concentrations were 0.7, 1.0, 1.6, 5, and 10 μM. The temperatures used were 10°C, 15°C, 20°C, 25°C, 30°C, 37°C, and 45°C. One set of experiments at a given temperature always included six cuvettes, five containing LDL and $CuSO_4$ and one containing LDL without $CuSO_4$. The recording of the 234 nm absorption was started immediately after the addition of $CuSO_4$ and continued in intervals of 4 or 6 min for periods up to 40 h depending on the oxidation rate. The recorded absorption data were finally processed by a computer to give the CD versus time curves (Fig. 1A, 2A) and the ΔA/min versus time curves (Fig. 1B, 2B). From these curves the lag time t_1, the time to reach $CD_{max/2}$ and CD_{max} (t_2 and t_3, respectively), the maximal rate of propagation v, and the CD_{max} were determined either graphically (lag time, see Fig. 3) or by using the Excel program (version 4.0).

Differential scanning calorimetry (DSC)

Calorimetry experiments were performed on the high-sensitivity differential adiabatic scanning microcal-

orimeter DASM-4 (Biobribor, Pushtchino, Russia) designed by Privalov (19). The scanning rate was 1°C/min. Samples with a concentration of 1 mg/mL of total LDL-cholesterol were loaded into the calorimeter sample cell at room temperature; an equal amount of buffer was loaded into the reference cell. The cells were pressurized by nitrogen to 2.5 bar to prevent loss of solvent by evaporation and formation of bubbles on heating. Data were collected on two heating runs. The first one from 1°C to 40°C, and the second from 1°C to 85°C. Samples were held at 1°C for approximately 30 min between the first and the second run. Each sample was scanned 2 or 3 times. The heat capacity versus temperature curves were interpreted in terms of the midpoint-temperature (T_m), taken as the temperature of the maximum change in heat capacity.

Data evaluation and statistics

The limiting values for the time indices, t_1* and t_2*, for the propagation rate v* and the associated constants K and K' were computed by a non-linear regression analysis using the Enzfit program (Fig. 4).

The temperature dependencies of all parameters were fitted by Arrhenius equation. Straight lines through the data were obtained with the method of least squares with the Excel program (version 4.0). Arrhenius plots were fitted by two models: *a)* linear dependency (no break point in one line) and *b)* change in linear

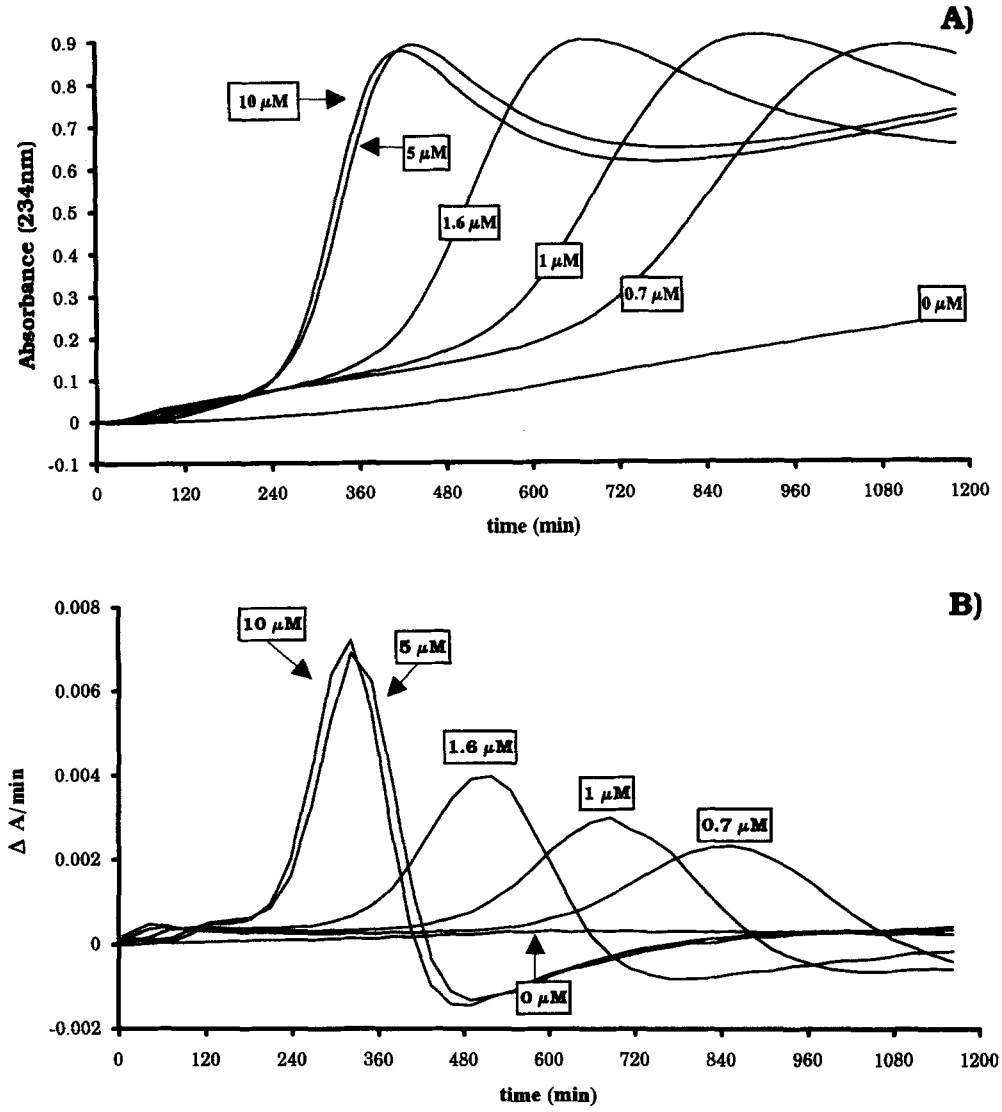

Fig. 1. Effect of Cu^{2+} on kinetics of LDL oxidation at 15°C. Six cuvettes containing 0.1 μM LDL in PBS were placed in the auto-cell holder, of a Beckman D-640 spectrometer and kept at 15°C. Oxidation was initiated by adding $CuSO_4$. The final copper concentrations were 10, 5.0, 1.6, 1.0, 0.7, and 0 μM. The oxidation was followed by recording the 234 nm absorption in each cuvette. A) Conjugated diene versus time curves (CD curves) B) First derivative of the CD curves representing the rate of oxidation as function of time.

dependency (by visual analysis) with break point resulting in two or three lines with different slopes. The fits for the different models (with or without break point) were statistically estimated by comparing the relative error sums of squares from the *F*-test for testing the goodness of fit. The apparent activation energy (E_a) was determined from the Arrhenius plots of rate of diene production v and from $1/t_l$.

RESULTS

Principle of determining the oxidation indices

The study of the effect of temperature on the kinetics of LDL oxidation was carried out by measuring the conjugated diene versus time curves (CD curves). **Figure 1** and **Figure 2** show as example two typical sets of LDL oxidation experiment, one at 15°C (Fig. 1) and the other at 45°C (Fig. 2). The upper part shows the CD curves obtained with different Cu^{2+} concentrations. The curves in the lower parts are the computed first derivatives of the CD curves and represent the rate of oxidation (ΔA/min) as a function of time. Consistent with a number of previous reports (6, 7) the CD curves showed three consecutive time phases: lag phase, propagation phase, and decomposition phase. During the lag phase, CD increased only slowly because lipid peroxidation is inhibited. In the subsequent propagation phase the lipid peroxidation is uninhibited and CD rapidly increases to a transient maximum (CD_{max}) of about 0.75 to 0.9

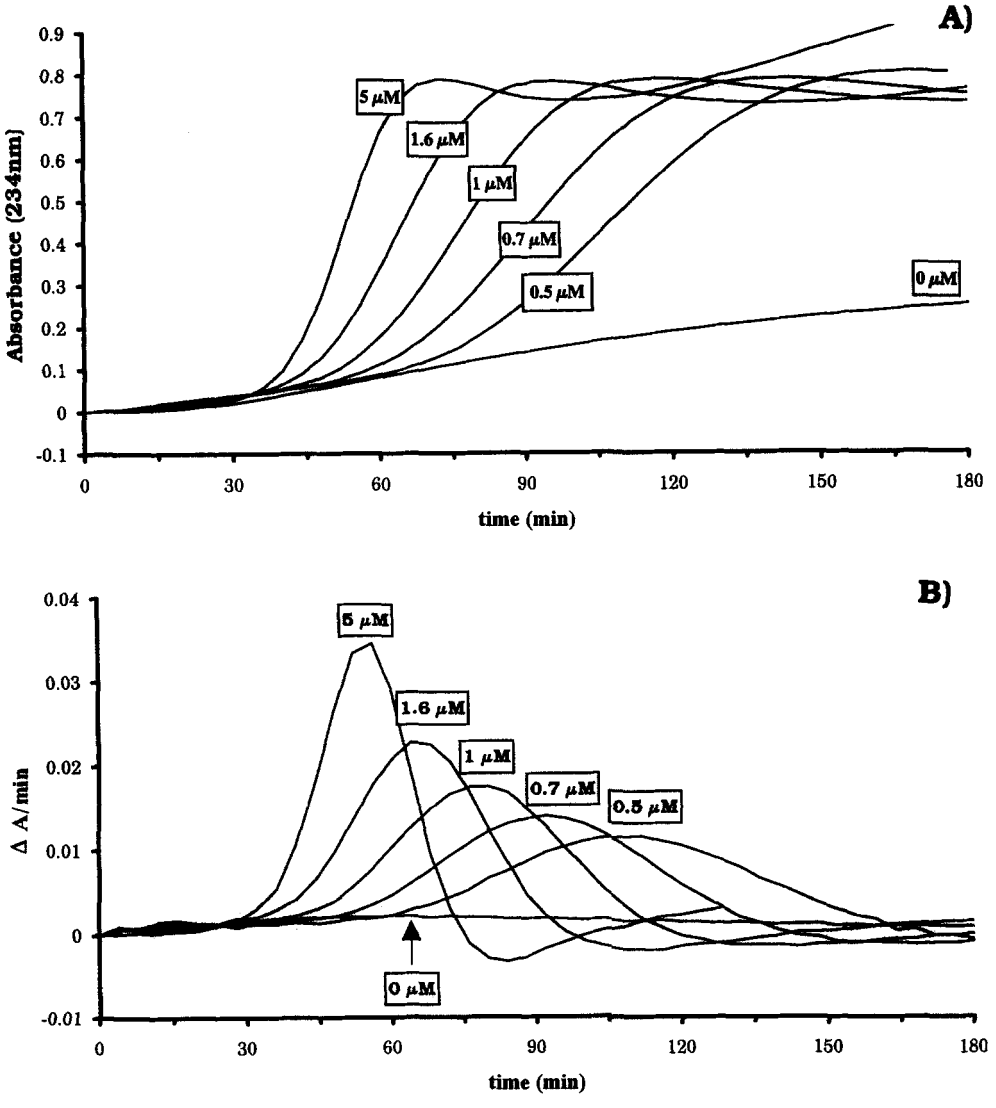

Fig. 2. Effect of Cu^{2+} on kinetics of LDL oxidation at 45°C. Experimental conditions as in Fig. 1, except that the autocell-holder was kept at 45°C and the final copper concentrations were 5.0, 1.6, 1.0, 0.7, 0.5, and 0 μM. A) Conjugated diene versus time curves (CD curves). B) First derivative of the CD curves. Note the different time scale between Fig. 1 and Fig. 2.

absorbance units. The CD curves show that the change of the 234 nm absorption during the decomposition phase is complex. The 234 nm absorption first decreased due to decomposition of CD and subsequently started to increase again. This second increase, however, is not due to newly formed lipid hydroperoxides with conjugated double bonds, but due to the accumulation of decomposition products with strong absorption in the 234 nm region. Some CD curves (e.g., Fig. 1A) did not exhibit the second increase because the experiment was terminated and the observation time was not long enough.

Several characteristic indices were obtained from each CD curve and the associated rate versus time curves. An example is shown in **Figure 3** for the oxidation of LDL in presence of 5 μM Cu^{2+} at 15°C and 45°C. The time indices t_1, t_2, and t_3 are the length of the lag phase (t_1), the time required to reach half maximum dienes (t_2), and the time to reach the diene peak (t_3), respectively. The maximal rate of propagation v is given by the peak in the ΔA/min curve. With a molar absorbance ε_{234nm} for conjugated dienes of 29,500 L mol^{-1} · cm^{-1} the rate of propagation in μM diene/min is given by 33.9 × ΔA/min. With an LDL concentration of 0.1 μM, as used in this study, the rate in mol diene formed per mol LDL and minute is equal to 339 × ΔA/min. Finally, the maximal concentration of dienes before the onset of decomposition was calculated from the absorbance A of the diene peak according to A × 33.9 (= μM dienes) or to A × 339 (= mol diene/mol LDL), respectively.

It is evident from the CD curves (Figs. 1, 2, and 3) that

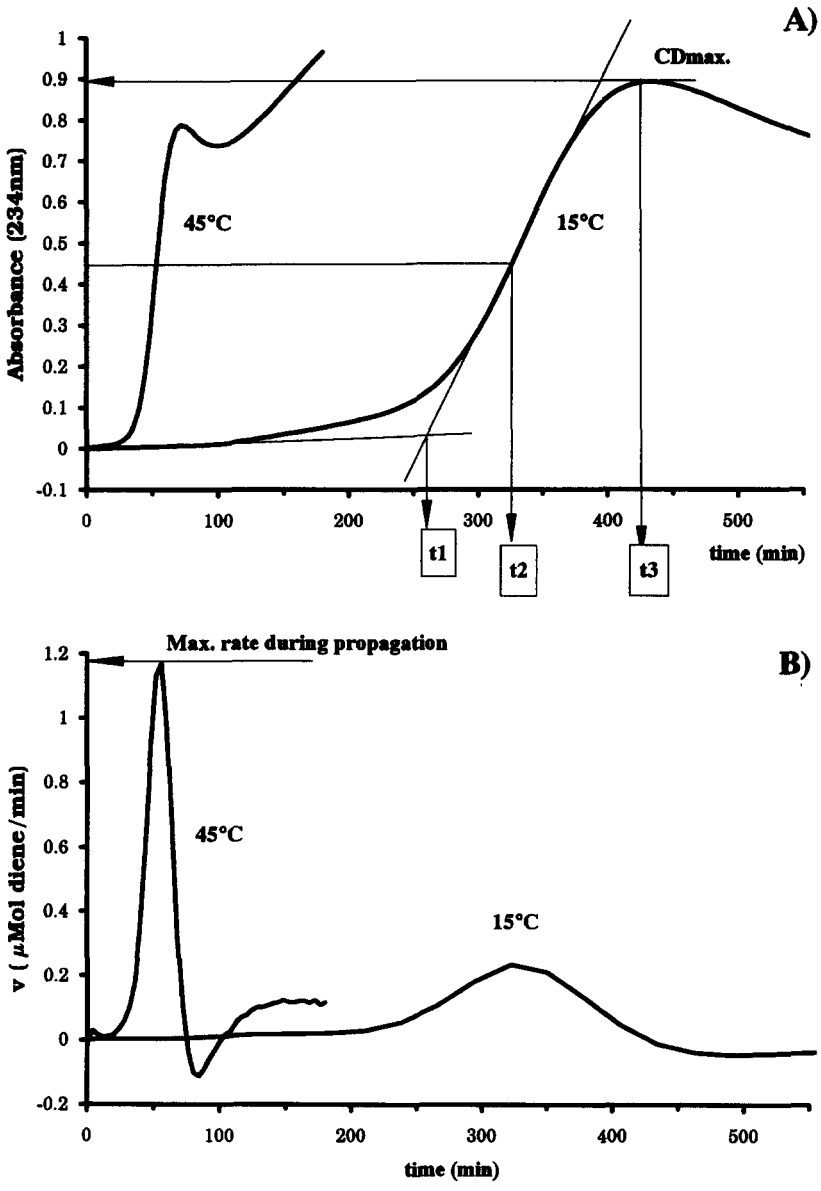

Fig. 3. Analysis of the CD curves to obtain the characteristic time indices. The curves are taken from Figs. 1 and 2 and show oxidation of LDL with 5 μM Cu^{2+} at 15°C and 45°C. A) The lag time t_1 is determined graphically by the intercept of the two tangents; t_2 (time to reach $CD_{max/2}$), t_3 (time to reach CD_{max}) and the CD_{max} value were computed from the data set using the Excel program version 4.0. B) The maximum propagation rate v is computed from the peak of the first derivative of the CD curves assuming a molar absorptivity for conjugated dienes of ε_{234} = 29 500 L • mol^{-1} • cm^{-1}; μM diene/min is equal to 33.9 × ΔA/min.

TABLE 1. Oxidation indices of LDL oxidation at 15°C and at 45°C

	15°C	45°C
Values for 5 μM Cu^{2+}		
t_1 (min), lag time	277	40.3
t_2 (min), time to reach $CD_{max/2}$	328	48
t_3 (min), time to reach CD_{max}	434	72
v (mol diene/mol LDL/min)	2.4	11.7
CD_{max} (mol diene/mol LDL)	302	267
Limiting values at Cu^{2+} > > 5 μM		
t_1* (min)	217.40 ± 7.82	35.30 ± 0.85
K (μM), Cu^{2+} where $t_1 = 2t_1$*	1.54 ± 0.09	0.57 ± 0.03
v* (mol diene/mol LDL/min)	3.07 ± 0.10	15.3 ± 0.50
K' (μM), Cu^{2+} where $v = v$*/2	1.84 ± 0.24	1.53 ± 0.05

Data are obtained from the LDL oxidation experiments shown in Fig. 1 (15°C) and Fig. 2 (45°C). The upper part of the table contains the indices at a $[Cu^{2+}] = 5$ μM (Fig. 3A and 3B). The lower part contains the computed limiting values for a $[Cu^{2+}] > > 5$ μM (Fig. 4). t_1 and t_1* are the lag time (t_1) and limiting lag time (t_1*); t_2 and t_3 give the time where conjugated dienes reach half maximum and maximum values, respectively. v and v* are, respectively, the propagation rate at 5 μM Cu^{2+} and the maximum propagation rate ($Cu^{2+} > > 5$ μM). CD_{max} gives the concentration of dienes in the LDL at the CD peak, i.e., before the onset of decomposition.

the time indices t_1, t_2, t_3 and the rate of propagation v were strongly dependent on both temperature and Cu^{2+} concentration, whereas CD_{max} was less dependent on these two variables. The oxidation indices obtained with 5 μM Cu^{2+} at 15°C and 45°C are summarized in **Table 1.** A 3-fold increase of temperature resulted in 7-fold decrease of t_1 and t_2; 6-fold decrease of t_3, and 5-fold increase in propagation rate v, whereas CD_{max} decreased only by 12%.

The curves in Figs. 1 and 2 further demonstrate that the oxidation indices converged to limiting values with increasing Cu^{2+} concentration. An example for this behavior is given for the lag time t_1 (**Fig. 4A**) and propagation rate v (Fig. 4B) at 15°C and 45°C. The dependence of t_1 from Cu^{2+} can be described by the equation 1:

$$t_1 = t_1^* \cdot K \cdot [Cu^{2+}]^{-1} + t_1^* \qquad \textit{Eq. 1)}$$

where t_1* is the limiting value of the lag time t_1 and K is the Cu^{2+} concentration for $t_1 = 2t_1$*. Using equation 1 and the measured t_1 values, non-linear regression analyses gave the respective values for t_1* and the associated constant K (Table 1). It should be noted that an alternative to non-linear regression analysis is to linearize the curves by plotting t_1 or t_2 versus $1/[Cu^{2+}]$ (7). The insert in Fig. 4A shows that the data points fit with straight lines, the intercept on the y-axis is t_1*, and the intercept on the x-axis is equal to $-1/K$.

The propagation rate v approached a maximal value with increasing Cu^{2+} concentration (Fig. 4B) and this relationship followed the equation 2:

$$V = V^* \cdot \frac{[Cu^{2+}]}{K' + [Cu^{2+}]} \qquad \textit{Eq. 2)}$$

where v* is the maximal rate of propagation and K' gives $[Cu^{2+}]$ for $v = v^*/2$. Using equation 2 and the experimental data sets for 15°C and 45°C, the v* and K' values listed in Table 1 were computed by non-linear regression analysis. The solid lines for lag time and propagation rate v (Fig. 4A, B) were computed with the respective constants listed in Table 1 and using equations 1 and 2, respectively. It is evident that there is an excellent agreement between the computed curves and the experimentally measured data points. A similar good fit was found for the other temperatures studied (data not shown). This clearly demonstrates that equations 1 and 2 describe adequately the dependence of the time indices and propagation rate from the Cu^{2+} concentration, at least in the range of 0.5 to 10 μM examined in this study.

Comparison of LDL prepared from fresh and stored plasma

To eliminate inter-subject variations of LDL from different donors, all measurements were done with samples prepared from one plasma pool. The plasma pool was prepared on one day from blood of nine donors. On the same day LDL was isolated from a portion of this pooled plasma and its oxidation indices were measured at 37°C (first column of **Table 2**). The remaining plasma was supplemented with sucrose, to prevent LDL aggregation, and stored in portions at -80°C. Whenever a new LDL sample was required during the course of this study, it was prepared from one of these aliquots. To definitely ensure that LDL prepared from the stored plasma always exhibits the same oxidation behavior, all oxidation indices were measured under the same conditions after 3, 6, 6.5, and 7.5 weeks of storage (Table 2). At the same temperature, another three oxidations of LDL were performed with this plasma pool; thus, in total, the oxidation indices at 37°C were measured 8 times. The respective mean values ± standard errors are summarized in the last column of Table 2. A comparison of the mean ± SE values with the individual measurement shows that all oxidation indices measured at the different time points were similar and were within the standard error of the assay. Also we measured the α- and γ-tocopherol content of fresh LDL and LDL from the stored plasma and the individual values were not different from the mean. From the data shown in Table 2 we conclude that storage of sucrose-containing EDTA-plasma at -80°C for up to 7.5 weeks does not change the oxidation behavior of LDL.

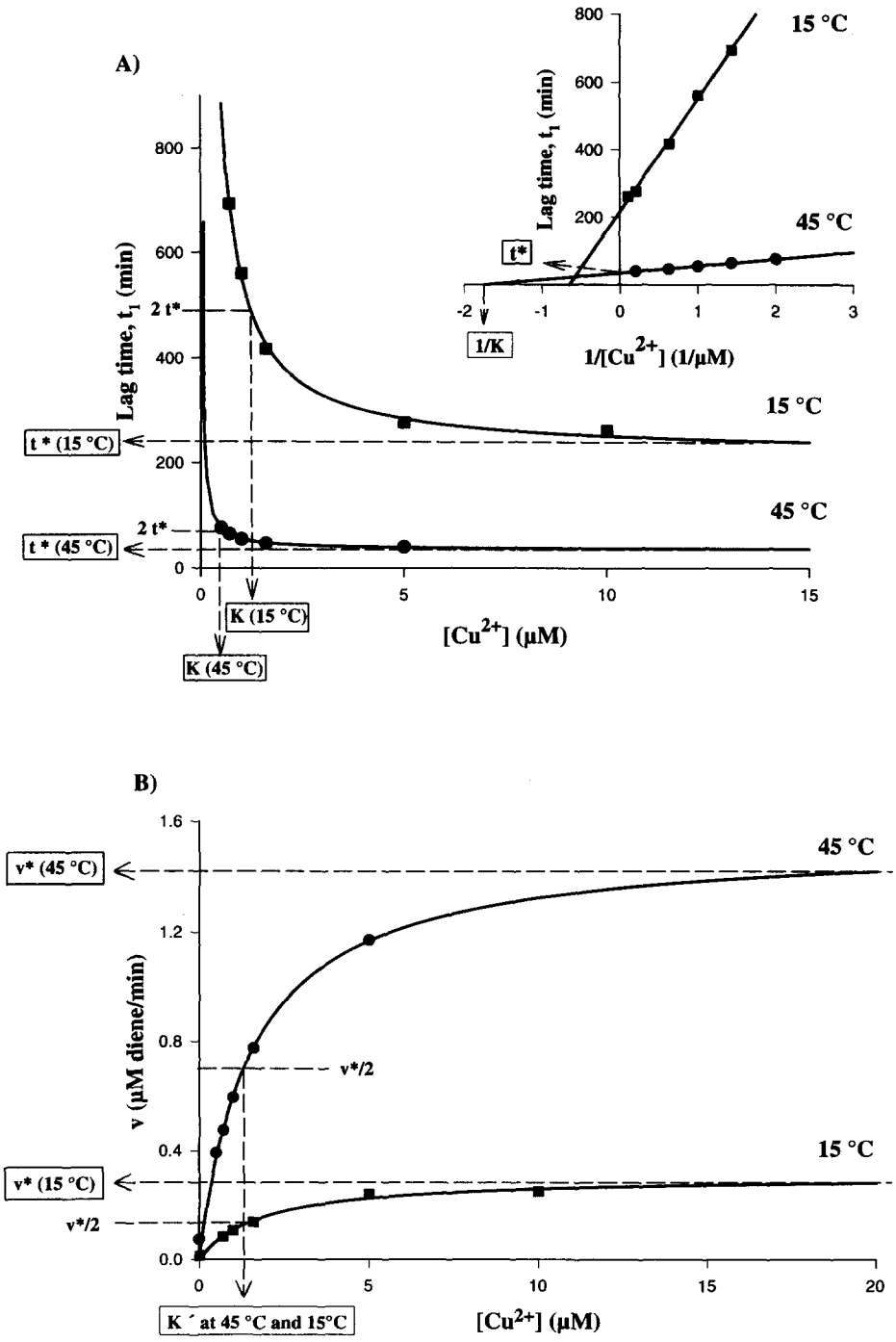

Fig. 4. Effect of Cu^{2+} on lag time t_1 and propagation rate v. Data points were obtained from Fig. 1 (15°C) and Fig. 2 (45°C). A) Effect of Cu^{2+} on lag time t_1. The solid lines were computed with equation 1 (see Results section), the respective values for K (that is $[Cu^{2+}]$ for $t = 2t^*$) and t^* were obtained by non-linear regression analysis. The insert shows the linearitiation by plotting lag time t_1 versus $1/[Cu^{2+}]$. B) Effect of Cu^{2+} on propagation rate v. The solid lines were computed with equation 2 (see Results section), the respective values for v^* and K' were obtained by non-linear regression analysis. The analysis was performed using the Enzfit program.

Phase transition of LDL

The measurements by differential scanning calorimetry (DSC) of the LDL used in this study showed a reversible core-lipid transition between 20°C↔37°C with a mid-point temperature (T_m) at 31.1 ± 0.2°C. The denaturation temperature of the apoB was found at 81 ± 0.2°C. In **Figure 5**, one of the calorimetric scans performed is shown as example.

TABLE 2. Effect of storage plasma at -80°C on oxidation resistance and vitamin E content of LDL

	Fresh Plasma	3 Weeks	6 Weeks	6 ½ Weeks	7 ½ Weeks	Mean Value ± SE
t_l (min), lag time	65	58	59	64	58	61.10 ± 2.14 (n = 8)
v (μM diene/min)	0.64	0.86	0.73	0.89	0.89	0.79 ± 0.04 (n = 8)
CD_{max} (mol diene/mol LDL)	271	285	240	282	266	277.00 ± 1.00 (n = 8)
K (μM)	1.11 ± 0.05	0.65 ± 0.10	0.79 ± 0.07	0.73 ± 0.08	1.10 ± 0.02	0.86 ± 0.07 (n = 7)
K' (μM)	2.13 ± 0.39	1.58 ± 0.10	2.01 ± 0.16	1.73 ± 0.15	1.92 ± 0.10	1.90 ± 0.24 (n = 7)
t_l* (min)	63.30 ± 9.00	49.10 ± 3.50	52.80 ± 2.20	57.10 ± 3.20	47.40 ± 0.50	52.30 ± 2.30 (n = 8)
v* (μmol diene/min)	1.08 ± 0.10	1.13 ± 0.03	0.89 ± 0.03	1.20 ± 0.05	1.24 ± 0.03	1.11 ± 0.05 (n = 8)
α-Tocopherol (mol/mol LDL)	6.00	5.44	–	5.55	5.49	5.29 ± 0.24 (n = 6)
γ-Tocopherol (mol/mol LDL)	0.23	0.3	–	0.21	0.32	0.28 ± 0.02 (n = 6)

The analyses were performed with LDL samples prepared from batches of a single plasma pool (1 mg/mL EDTA, 0.6% sucrose) used fresh or stored at -80°C for the indicated time periods. The oxidation indices t_l, v, and CD_{max} were obtained from CD curves recorded at 37°C with 0.1 μM LDL and 5 μM Cu^{2+}. The limiting values t_l* and v* and the associated constants K and K' were calculated by non-linear regression analyses. Vitamin E content was measured before oxidation in all the points but in the one at 6 weeks. The mean ± SE include the listed experiments plus two to three additional experiments (n = 6 to 8).

Temperature dependence of the time indices, rate of propagation, and diene maximum

To obtain the temperature dependence of LDL oxidation, the CD curves were measured at 10, 15, 20, 25, 30, 37, and 45°C with five different Cu2+ concentrations, each ranging from 0.5 to 10 mM. As shown in the **Figure 6**, both lag times t1 and t2 decreased with increasing temperature whereas rate of propagation v increased (**Fig. 7A**). The change was not linear but rather exponential. However, this effect was not the same for all the [Cu2+] studied, indicating that the effect of temperature on lag time is also strongly dependent on copper. In fact, the temperature dependence of t1 and t2 was more pronounced at low Cu2+ concentrations; for example, with increasing temperature from 10°C to 45°C the decreases observed in t1 were 8.8%, 14.2%, 16.7%, and 20.2% for 5.0, 1.6, 1.0, and 0.7 mM Cu2+, respectively.

The plot of log v versus the reciprocal absolute temperature gave strict linear relationships for all copper concentrations (**Fig. 8A**). The temperature dependence of the rate of propagation, therefore, fully obeys the Arrhenius law in the temperature range of 10°C to 45°C and is not influenced by the phase transition of LDL used in this study.

The reciprocal value of the lag time t1 was assumed

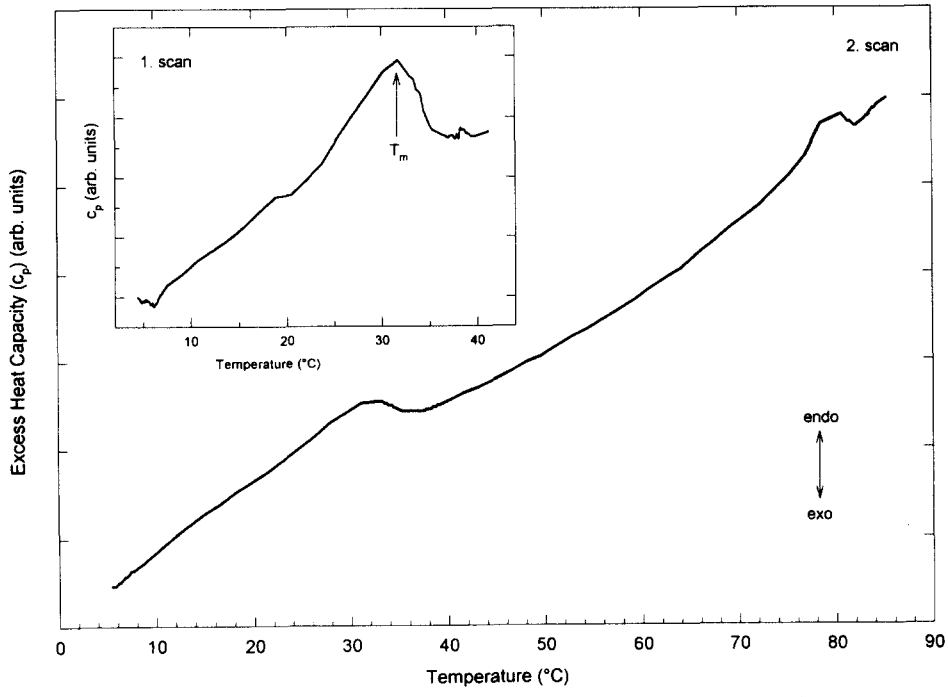

Fig. 5. Determination of phase transition of LDL by differential scanning calorimetry (DSC). One representative DSC-thermogram (not baseline corrected, not normalized) within the temperature range of 1°C to 85°C (2. scan) is shown. The inset (1.scan) shows the head capacity function (c_p) versus temperature (baseline subtracted, not normalized) within the temperature range of 1°C to 40°C. ↑ means that reaction is endothermic. The mid-point temperature T_m for core transition is 31.1°C.

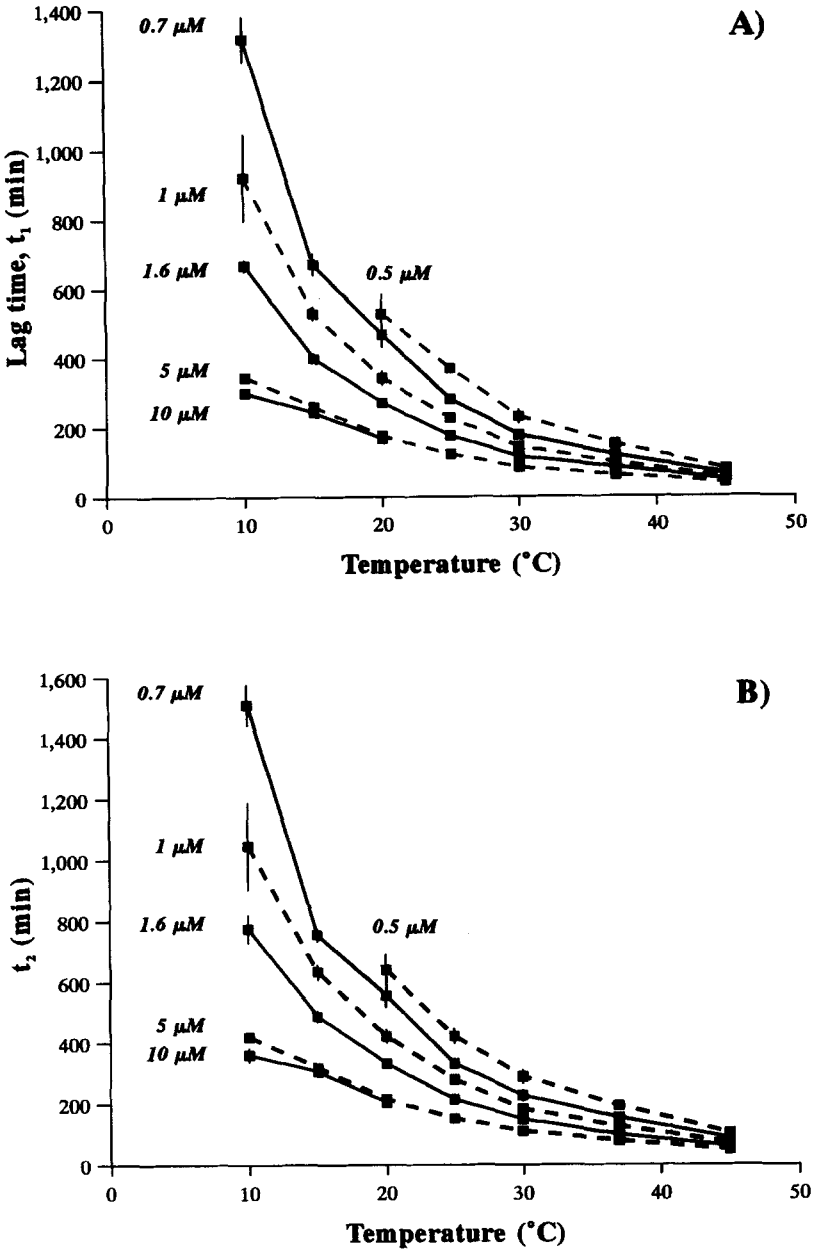

Fig. 6. Influence of temperature on A) lag time t_1 and B) the time t_2 to reach $CD_{max/2}$. The time indices for each temperature were obtained from CD curves with different Cu^{2+} concentrations. All experimental conditions are the same those in Figs. 1 and 2. All the data points are mean ± SE of three to eight independent experiments.

dation is initiated (20). The Arrhenius plots of log $1/t_1$ versus the reciprocal absolute temperature (Fig. 8B) again gave strict linear relationships for oxidations with 0.5, 0.7 and 1 μM Cu^{2+}. In the experiments with 1.6 and 5 μM Cu^{2+}, the 30°C values were slightly outside the straight lines computed by the method of least squares. The plots of t_2 (log $1/t_2$ versus $1/T$) gave similar results (data not shown). Taken together, the Arrhenius plots of the time indices suggest that the phase transition may have a small effect on lag time, when oxidations are carried out with Cu^{2+} concentrations of 1.6 μM or higher.

The maximal amount of dienes (CD_{max}) decreased slightly with increasing temperature. The highest value was 345.1 ± 5.8 mol diene/mol LDL at 10°C and the lowest 267.2 ± 1.6 mol diene/mol LDL at 45°C (**Table 3**). This change of only 23% is much less than the changes observed for t_1, t_2, and *v*. The CD curves for 15°C and 45°C (Figs. 1, 2) suggest that CD_{max} is independent of the concentration of copper. The same behavior was found for all other temperatures and proves that CD_{max} has a constant value at a given temperature. The low standard deviation of CD_{max} shows that this value can be measured in a highly reproducible manner. In the Arrhenius plots (log CD_{max} versus $1/T$) all data points were on a straight line.

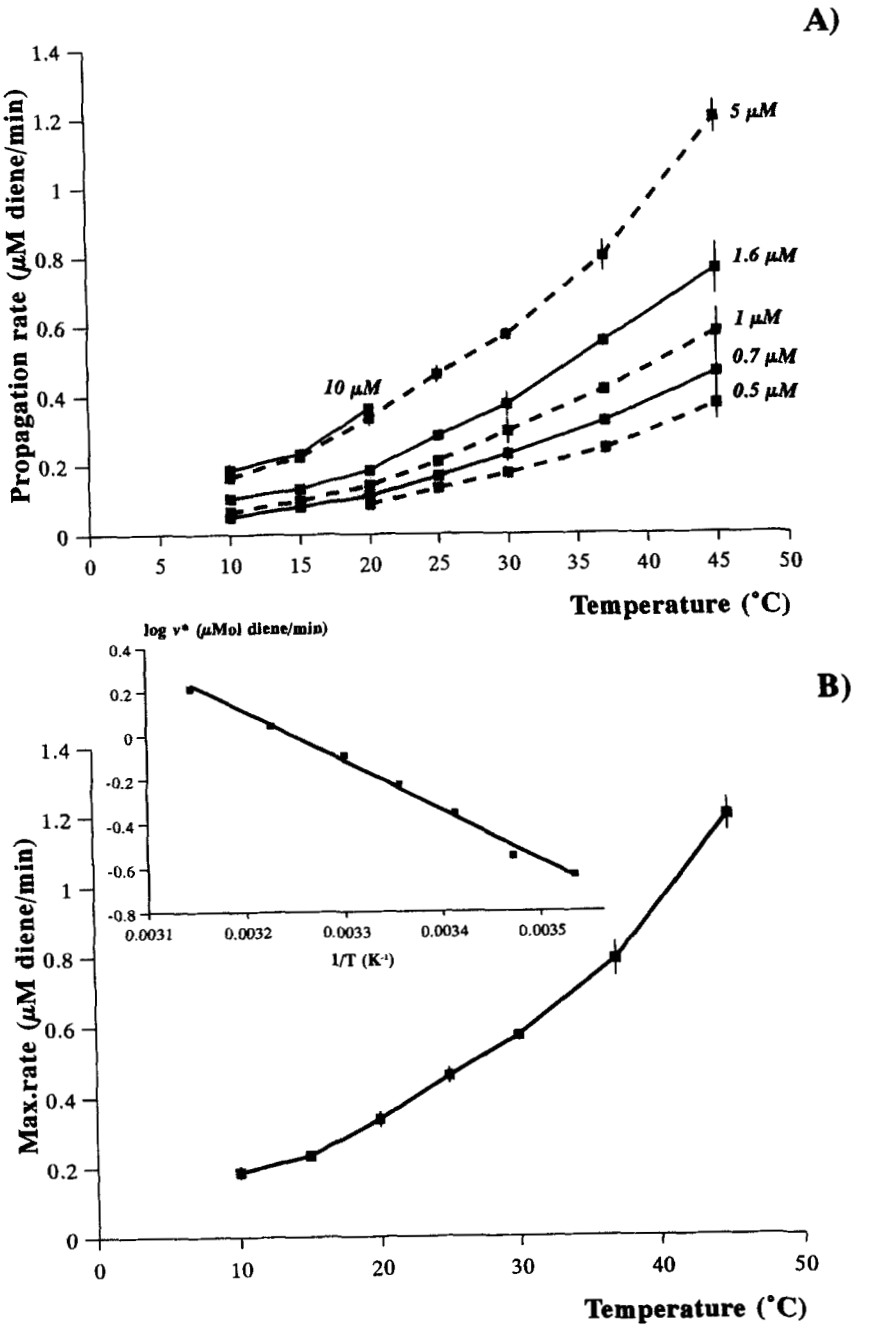

Fig. 7. Influence of temperature on the propagation rate *v*. A) Propagation rate (μM diene/min) experimentally determined for each temperature with different copper concentration. B) Extrapolated maximum propagation rate v^* with excess Cu^{2+} at each temperature. The values were computed with a non-linear regression analysis using equation 2 and the data set shown in Fig. 7A. The insert shows the Arrhenius plot for v^*. The straight line drawn through the data points was obtained by a method of least squares. All the data points shown in A and B are the mean ± SE of three to eight different experiments; where no error bar is shown, the SE was smaller than the size of the symbol.

Temperature dependence of the constants in equations 1 and 2

In the previous section it has been shown for 15°C and 45°C (Table 1, Fig. 4) that the time indices approached minimum values with increasing Cu^{2+} concentration, whereas rate of propagation approached a maximum value. The same behavior was found for all other temperatures studied (graphs not shown). Using equations 1 and 2 the magnitude of the limit values for lag time (t*) and for propagation rate (v^*) and the associated constants K and K' were determined for each temperature by non-linear regression analyses. Sub-

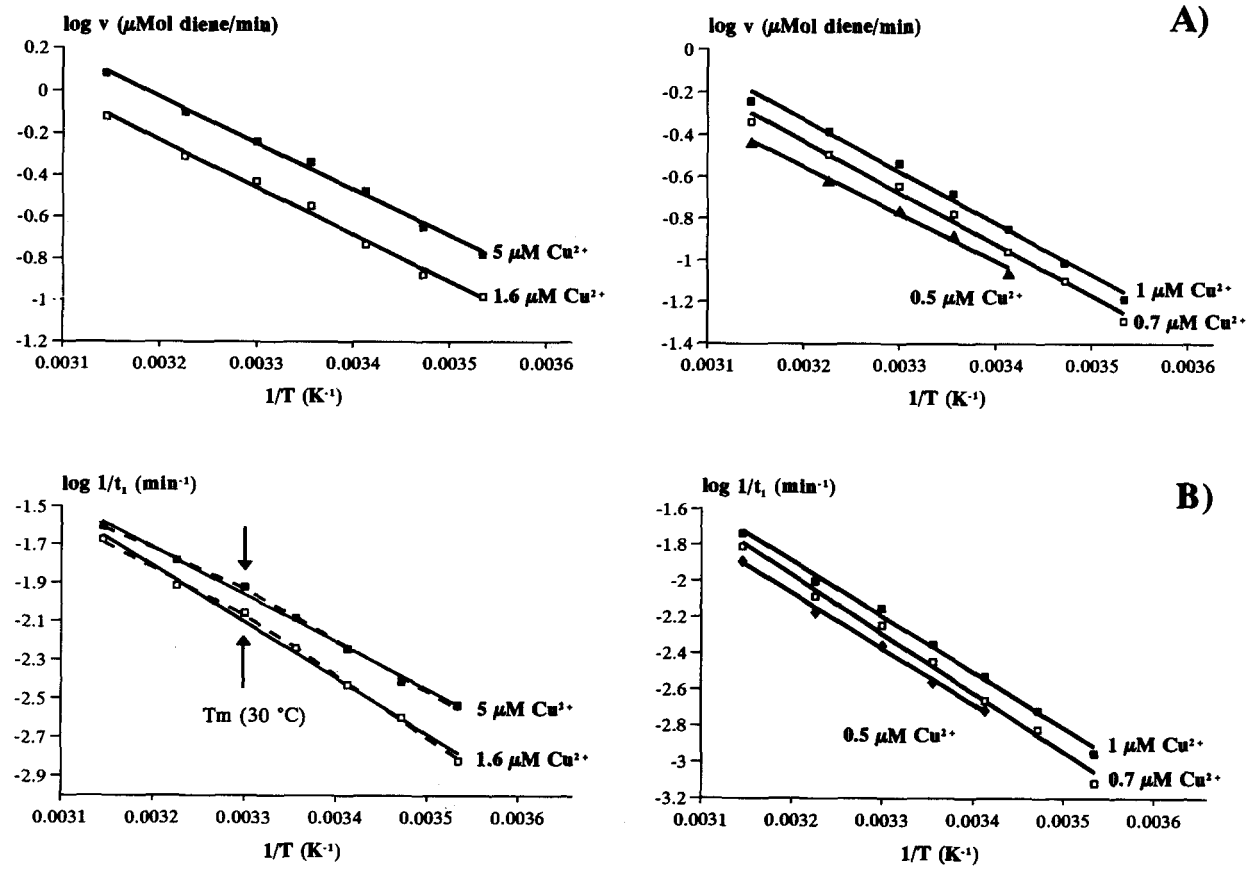

Fig. 8. Arrhenius plots of the propagation rate v and lag time t_1. A) Arrhenius plots for propagation phase at different copper concentrations (the data plotted as log v versus 1/T were taken from Fig. 7A). The straight lines drawn through the data points were obtained by the method of least squares. The models are supported by the analysis of the residuals and by the F-test for goodness of fit. B) Arrhenius plots for lag phase at different copper concentrations (the data plotted as log 1/lag time versus 1/T are from Fig. 6A). For 5 and 1.6 μM Cu^{2+} the model without the break points gave a better fit statistically and is represented by solid line; the model with discontinuities is drawn by a dashed line. The possible breaks in the Arrhenius plots for 5 and 1.6 μM Cu^{2+} are shown by arrows.

sequently, the temperature dependence of t* and v* was analyzed graphically. The plots in **Fig. 9** show that t_1*, t_2* steadily decreased above 15°C, but the values for 10°C were identical with the values at 15°C (no statistical differences were found when the data were analyzed by Student's t test). The analyses of the t_1* data by an Arrhenius plot are shown in the insert of Fig. 9. The solid line represents the computed linear relationship with the best fit for all the data. Although the data points fit rather well with a straight line, it is possible that there are breaks (indicated by an arrow) around 15°C and 30°C. The Arrhenius plot of t_2* was similar with two possible breaks at 30°C and 15°C (data not shown).

TABLE 3. Effect of temperature on maximal amount of dienes present in LDL before onset of decomposition

Temperature	CD_{max}	% of Decrease versus Maximum Value
C	*mol diene/mol LDL*	
10	345.05 ± 5.82	0
15	312.66 ± 2.39	9
20	315.09 ± 2.62	9
25	306.08 ± 2.68	10
30	297.91 ± 4.24	14
37	277.25 ± 1.27	20
45	267.16 ± 1.58	23

CD curves were recorded at the indicated temperatures with 0.1 μM LDL and different Cu^{2+} concentrations as shown in Fig. 1. The diene content of LDL was calculated from the diene peak (CD_{max}). The values listed are the mean ± SE of the five experiments with different Cu^{2+} concentrations.

Figure 7B shows that v* steadily increased with increasing temperature. This temperature dependence strictly followed the Arrhenius law as shown by the linear relationship between log v* and 1/T (insert of Fig. 7B).

We also analyzed the temperature dependence of the constants K and K' (equation 1, equation 2). The magnitude of these values represents the Cu^{2+} concentrations, where t = 2t* (K) and $v = v^*/2$ (K'), respectively. The magnitude of the K values was determined from the lag time data t_1 and the K' values were determined from the rate data (v). The temperature dependence of K clearly exhibited three consecutive phases, **Fig. 10**, first (10–15°C) a rapid drop, then a range (15–30°C) where

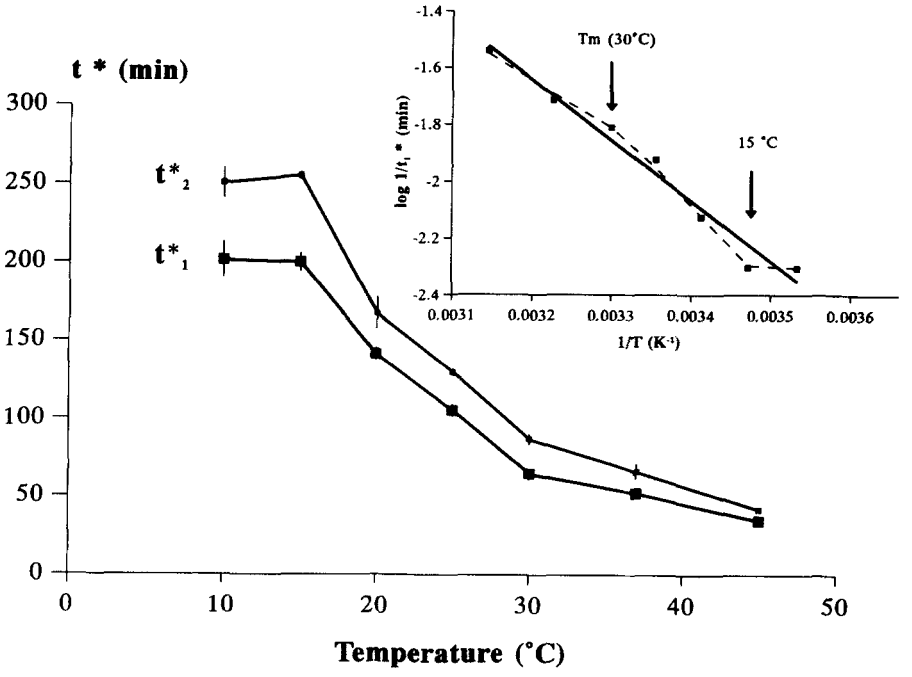

Fig. 9. Influence of temperature on the limiting values of the lag time t_1* and time to reach $CD_{max/2}$ (t_2*). The values t_1* and t_2* were obtained by non-linear regression analyses using equation 1 and the data set shown in Fig. 6A and B. All the data points are mean ± SE of 3–8 different experiments; where no error bar is shown, the SE was smaller than the size of the symbol. The insert shows an Arrhenius plot as log $1/t_1$* versus $1/T$. The straight line drawn through the data points was calculated by the method of least squares.

the value remains more or less constant, and then a second phase of decrease (30–45°C). An Arrhenius plot (log K versus $1/T$) shows these three temperature ranges even more pronounced with clear breaks at 15°C and 30°C (Fig. 10 inset). These results show that the temperature dependence of the K value mimics the temperature dependence of t_1* and t_2*, which also showed, though less pronounced, breaks at 15°C and 30°C (Fig. 9). The second break agrees well with the mid-point temperature (T_m = 31.1°C) of the phase transition of the LDL used in this study. The calorimetric curves (Fig. 5), however, did not show a peak around 15°C.

The magnitude of the K' constant (equation 2) as shown in **Table 4** was almost the same for all temperatures with a value of 1.95 ± 0.08 μM (mean ± SE, n = 27) suggesting that this constant is temperature independent.

Activation energy of copper-mediated LDL oxidation

A plot of the logarithm of the reaction rate against the reciprocal of the absolute temperature (1/T), should give a straight line with a slope equal to $E_a/2.303$ R, where E_a is the apparent activation energy in cal/mol and R is the gas constant (R = 1.987 cal · K^{-1} · mol^{-1}). We first analyzed the data set (10–45°C) for propagation rate v and found that the temperature dependence of the propagation rate obeys the Arrhenius equation (Fig. 8A). Moreover, all five copper concentrations (0.5, 0.7, 1.0, 1.6, and 5.0 μM) and the plot of log v* for Cu^{2+} concentration > > 5 μM (Fig. 7A inset) gave lines with equal slopes indicating that the E_a for propagation was independent on the concentration of Cu^{2+} used to oxidize LDL. The computed mean activation energy for the propagation rate v was 10.61 ± 0.22 kcal/mol (mean ± SE) with a coefficient of variation between the E_a at different Cu^{2+} concentration < 5%. The individual values of E_a measured from v at the different Cu^{2+} concentrations are listed in **Table 5.**

If lag time t_1 is inversely proportional to rate of initiation, the temperature dependence of the reciprocal lag time should give the activation energy of initiation. The plots of log $1/t_1$ versus $1/T$ (Fig. 8B) demonstrate that the data are compatible to a large extent with straight lines as predicted by the Arrhenius equation. The computed mean activation energy for initiation is 12.9 ± 0.83 kcal/mol (mean ± SE). These Arrhenius plots, ascribed with lag phase, showed different slopes depending on the copper concentration. With the high Cu^{2+} concentrations (1.6, 5, and > > 5 μM Cu^{2+}) the computed activation energy was 11.4 ± 1.0 kcal/mol (mean ± SE) and with the low Cu^{2+} concentrations (1.0, 0.7, and 0.5 μM) was 14.4 ± 0.3 kcal/mol (mean ± SE). The individual values of E_a measured from 1/lag time at the different Cu^{2+} concentrations are listed in Table 5.

A more rigorous analysis suggests that values for

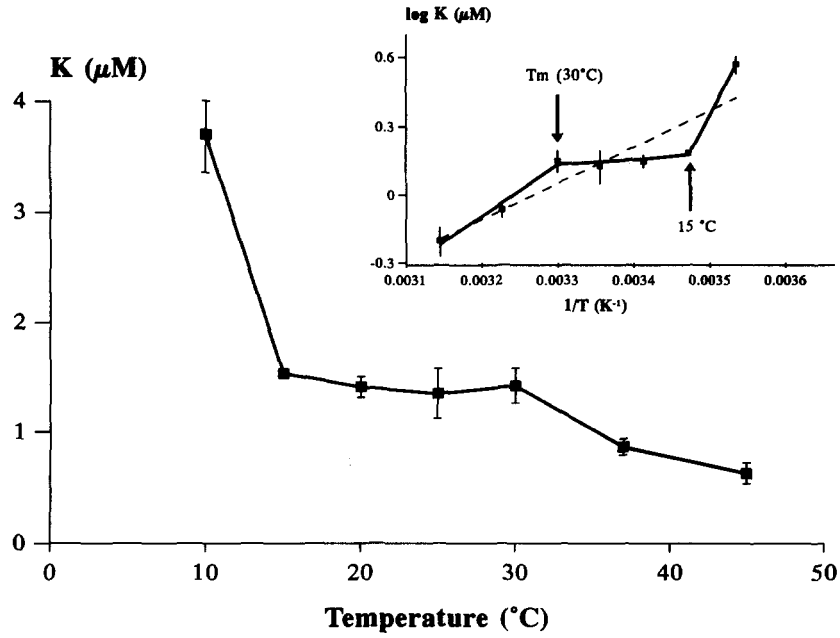

Fig. 10. Influence of temperature on the copper binding constant *K*. The values of the constant *K* were computed with equation 1 using the data set shown in Fig. 6A. All the data points are mean ± SE of 3–8 different experiments. The insert shows the Arrhenius plot for *K* values as log *K* versus 1/T. The straight lines drawn through the data points were obtained by the method of least squares. The models are supported by the analysis of the residuals and by the F-test for goodness of fit; the model with the break points gave a significantly better fit and is represented by a solid line; the model without discontinuities is drawn by a dashed line. The breaks in the Arrhenius plots are shown by arrows.

concentrations of 1.6, 5 (Fig. 8B) and > > 5 μM Cu^{2+} (Fig. 9 inset) are indeed composed of two straight lines with different slopes and an intercept at 30°C, the transition temperature of LDL. With the two-line model the activation energy for initiation above the transition temperature T_m would be lower (~9.7 kcal/mol) as compared to temperatures below the T_m (~13.2 kcal/mol).

DISCUSSION

The main goal of this study was to clarify the role of temperature and phase transition on the oxidation behavior of LDL in presence of Cu^{2+} ions. Human LDL exhibits a reversible phase transition in the temperature range of 20°C to 40°C, depending on the triglyceride content (11, 13, 14). It is believed that the phase of the core lipids (cholesteryl ester, triglycerides) changes above a critical temperature (= melting point) from an ordered smectic liquid-crystalline to a disordered liquid-like state. The structure of apoB is presumed to be insensitive to the core transition (21) and no major conformational changes of apoB were observed in the range of 0°C to 70°C (16). However, that does not exclude the possibility that phase transition affects Cu^{2+} binding and the oxidizability of the LDL lipids. For example, studies on Mn^{2+} binding of porcine LDL indicate that metal ion binding properties of LDL are influenced by core transition (13).

TABLE 4. Effect of temperature on the constant *K'*

Temperature	*K'*
°C	μM
10	2.33 ± 0.18
15	1.88 ± 0.06
20	2.15 ± 0.11
25	1.84 ± 0.11
30	1.86 ± 0.03
37	1.90 ± 0.24
45	1.71 ± 0.25
Mean ± SE	1.95 ± 0.08

K' constant, that is [Cu^{2+}] for $v = v^*/2$, was computed with equation 2 using the data shown in Fig. 7A. The values listed are the mean ± SE of the three to seven independent experiments.

As measurements of the oxidation resistance of LDL are carried out at temperatures between 20°C to 37°C, it might well be that the variability of the oxidative resistance of LDL from different subjects and of different LDL subfractions (10) is, in part, due to differences in the LDL "melting point." The calorimetric phase transition of the LDL sample used in this study occurred at a mid-point temperature T_m (melting point) of 31.1°C (Fig. 5) which is in good agreement with T_m values reported by others (11, 12, 22).

We have shown here for the first time that the temperature dependence of LDL oxidation is primarily governed by the Arrhenius law, which links the rate of

TABLE 5. Apparent activation energies (E_a) for lag phase and propagation phase during Cu^{2+}-mediated oxidation of a pool-LDL

	E_a	
$[Cu^{2+}]$	Lag Phase Obtained from t_l	Propagation Phase Obtained from v
μM	*kcal/mol*	
0.5	14.21	10.36
0.7	14.93	11.26
1.0	14.08	11.30
1.6	13.30	10.35
5.0	11.20	10.10
Mean ± SE (n = 5)	13.54 ± 0.64	10.67 ± 0.25
> > 5	9.70	10.30
Mean ± SE (n = 6)	12.9 ± 0.83	10.61 ± 0.22

The values were obtained from the different plots shown in Fig. 8 and in the insets of Figs. 7A and 9B, taking into account that the slope of the lines is equal to $E_a/2.303\ R$, where R is the gas constant (1.987 cal/*K*/mol).

a chemical reaction with its activation energy (E_a) and the absolute temperature: $v = B \cdot e^{-Ea/RT}$ where B is a constant. Effects of phase transition on rate of LDL oxidation should reveal a biphasic Arrhenius plot with a break at or close to the transition temperature. Such biphasic Arrhenius plots were frequently observed in membrane-bound enzymes and often ascribed to lipid transition and changes in phospholipid–protein interactions. Different explanations have been suggested for each individual enzyme. One possible cause for non-linear Arrhenius plot is a temperature-dependent structural transition (23).

A rate that can be readily obtained from the conjugated diene versus time curves (Figs. 1, 2) is the maximum propagation rate v (Fig. 3B). Rising temperature caused a strong increase in propagation rate (Fig. 7A). The lowest rate was 0.05 μM dienes/min (observed at 10°C with 0.7 μM Cu^{2+}) and the highest rate was 1.2 μM dienes/min (45°C and 5 μM Cu^{2+}). The Arrhenius plots of log v versus 1/T (Fig. 8A and Fig. 7B inset) prove three important points. *a)* The temperature dependence of the propagation rate is solely governed by the Arrhenius law. *b)* The transition temperature has no effect whatsoever on the propagation rate, as the plots show no break around 30°C. The most reasonable explanation for that is that the accumulated lipid peroxidation products minimize the effects of core transition on propagation rate even if this order–disorder transition is evident in oxidized LDL (22). *c)* The activation energy of the reaction controlling the propagation rate is 10.61 kcal/mol (Table 5). This activation energy is not influenced by the Cu^{2+} concentration as the plots for 0.5 to 5 μM Cu^{2+} (Fig. 8A) and for excess Cu^{2+} (inset of Fig. 7B) gave exactly the same slope. This quantity for the activation energy can be considered as a characteristic value that could provide important clues on the mechanism of LDL oxidation, particularly on the transition state of the reacting molecules. However, we frankly admit that our knowledge of the theory of reaction kinetics and thermodynamics is not sufficient to give a reasonable interpretation.

Consistent with previous studies (8, 24) we found that the lag time decreased with increasing temperature. The longest lag time in our study was 21.9 h (0.7 μM Cu^{2+}, 10°C) and the shortest one was 40 min (5 μM Cu^{2+}, 45°C). As only subtle compositional changes take place in LDL during the early phase of oxidation (i.e., oxidation of vitamin E, formation of a few molecules of lipid hydroperoxides), and based on previous studies with two LDL subfractions (10), we expected that the phase transition at 30°C would have a marked effect on lag time in our LDL sample. Surprisingly, this was not the case. The Arrhenius plots of the reciprocal lag time (log $1/t_l$) versus 1/T at all five copper concentrations again gave almost straight lines with $r = 0.98$ or better (Fig. 8B). An only exception was the plot of the minimal lag time t_l* extrapolated for large excess of copper (> > 5 μM), which exhibited two possible breaks around 15°C and 30°C (Fig. 9 inset).

These results clearly show the following. *a)* The temperature dependence of the rate of initiation (defined as reciprocal of lag time) obeys the Arrhenius law over a wide range with no clear discontinuities even at high Cu^{2+} concentration. *b)* Phase transition of LDL has no measurable effect on rate of initiation (or lag time) as the Arrhenius plots do not show a break around 30°C. Exception for this rule, however, may become evident if LDL is oxidized with a very large excess of Cu^{2+}. *c)* The initiation reaction has an average activation energy of about 13 kcal/mol (Table 5). The value results from the averaged slopes of the Arrhenius plots (possible breaks not considered) measured at different Cu^{2+} concentrations. This value is clearly higher than the activation energy for propagation, suggesting that the rate limiting reactions during the two phases are different.

The data set obtained in this study also enabled us to analyze for the first time the copper binding constants and their temperature dependence. At all temperatures the dependence of the propagation rate from the copper concentration obeyed exactly the saturation function given by equation 2, which has the same form as the Michaelis-Menten equation. One possible interpretation for this relationship is that the apolipoprotein B behaves like an apo-enzyme which gains a catalytic prooxidative activity through binding of Cu^{2+} ions (= cofactor). The LDL–Cu^{2+} complex would then represent a holoenzyme capable of oxidizing the LDL lipids. A kinetic treatment of such a model results in equation 2 with K' as dissociation constant of the LDL–Cu^{2+} com-

plex. The dissociation constants K' determined for the various temperatures were nearly identical (Table 4) with a mean ± SD of 1.95 ± 0.39 μM Cu^{2+}. This proves that phase transition has no effect whatsoever on the LDL–Cu^{2+} complex mediating propagation. For clarity it should be mentioned that K' = 1.95 μM means that half maximal rate of propagation ($v = v^*/2$) is reached at a Cu^{2+} concentration of 1.95 μM, or, in other words, a ratio of 19 Cu^{2+}/LDL particle is necessary for 50% saturation of the prooxidative binding sites. Half maximal oxidized LDL (measurement of K') is likely in such a disordered state that effects of temperature on the lipid phase, apoB structure, and Cu^{2+}-binding sites are negligible and hence K' remains almost constant between 15°C to 45°C.

The dependence of the lag time t_1 from the Cu^{2+} concentration followed equation 1 at each temperature. With the assumption that the reciprocal lag time is proportional to the rate of initiation ($R_i \sim 1/t_1$) this equation obtains the same form as the rate equation 2 and links rate of initiation R_i with the copper concentration.

$$R_i = R_{i\,max} \cdot \frac{[Cu^{2+}]}{K + [Cu^{2+}]} \qquad \textit{Eq. 3)}$$

where K value is the Cu^{2+} concentration at which rate of initiation is half maximal ($R_i = R_{imax/2}$). The temperature dependence of K value (Fig. 10) and more pronounced the Arrhenius plot of log K versus 1/T (inset Fig. 10) showed breaks at 15°C and at 30°C, the melting point of the LDL sample.

Thus it appears that the only two parameters sensitive to thermal transition are the constant K (Fig. 10 inset) and to a lesser extent R_{imax} (defined as reciprocal minimal lag time, Fig. 9 inset). We assume that LDL has a limited number of prooxidative Cu^{2+} binding sites (7, 20, 24). Some of these binding sites are most likely located at the periphery of apoB, close to tryptophane residues (25). In the temperature range of 15°C to 30°C, initiation and propagation appear to be mediated by the same type of Cu^{2+} complex as the measured dissociation constants (mean ± SD) are almost equal K = 1.43 ± 0.26 μM (n = 14) and K' 1.94 ± 0.20 μM (n = 14). It is reasonable to assume that core melting at 31°C causes structural changes in the apoB that increase the accessibility of Cu^{2+} binding sites (decrease of K value) whereas lowering temperature below 15°C probably causes structural changes in the microenvironment of the binding sites making a few or all of them somewhat less accessible for Cu^{2+} (increase of K). The existence of such a second thermal transition below the core melting temperature is consistent with an observation made by Herak et al. (13) in porcine LDL, where they found that some changes of the surface occur below phase transition of the core. These changes affect Mn^{2+} binding but are not associated with significant heat exchange measured by calorimetry. ESR spectroscopy also suggests the coexistence of two components in the monolayer with different mobility (26). Perhaps one of these components becomes immobilized below 15°C and thereby induces changes in the interaction of the monolayer with apoB, which in turn affect metal ion binding.

It is well known that the oxidation behavior of LDL samples from different donors varies significantly, even when measured under strictly standardized conditions. These variations were ascribed to differences in the content of antioxidants, polyunsaturated fatty acids, preformed peroxides, and other factors such as heterogeneity in particle size. It cannot be excluded that defined LDL subfractions show the effect of core melting more pronounced than pool-LDL containing all different LDL subfractions. However, this study (involving a large number of representative measurements) on the temperature and Cu^{2+} dependence of LDL oxidation would not have been possible without having a larger quantity of LDL at hand showing constant oxidation properties over a longer period of time. We think that we have solved this problem successfully by using a frozen (-80°C) plasma pool as the source of a "standard LDL." As the pool was prepared from nine clinically healthy normolipidemic subjects, the results should represent characteristic average values. Consistent with that, oxidation indices determined at a temperature of 30°C were in the range of values found previously with other LDL samples (7). It is also important that EDTA-plasma supplemented with 0.6% sucrose can be stored at -80°C for at least 2 months without a change in the oxidation behavior of LDL (Table 2). This is in full agreement with the observation by Kleinveld et al. (9) and Gieseg and Esterbauer (7), who stored plasma under the same conditions for 5 weeks and 2 weeks, respectively. The ability to store plasma has many advantages in designing the logistics of epidemiological or clinical studies, where a larger number of LDL samples must be analyzed.

The authors' work has been supported by the FWF projects no. SO 7102-Med and no. P10105-MOB; Pilar Ramos was supported by a Lise-Meitner-Fellowship no. MO152-CHE from The Austrian Science Foundation. We thank Karin Goldner for her helpful assistance.

Manuscript received 1 March 1995.

REFERENCES

1. Steinberg, D., S. Parthasarathy, T. E. Carew, J. C. Khoo, and J. L. Witztum. 1989. Beyond cholesterol. Modifications of low-density lipoprotein that increase its athero-

genicity. *N. Engl. J. Med.* **320:** 915–924.
2. Esterbauer, H., J. Gebicki, H. Puhl, and G. Jürgens. 1992. The role of lipid peroxidation and antioxidants in oxidative modification of LDL. *Free Radical Biol. Med.* **13:** 341–390.
3. Salonen, J. T., S. Ylä-Herttuala, R. Yamamoto, S. Butler, H. Korpela, R. Salonen, K. Nyyssonen, W. Palinski, and J. L. Witztum. 1992. Autoantibody against oxidised LDL and progression of carotid atherosclerosis. *Lancet.* **339:** 883–887.
4. Jessup, W., S. M. Rankin, C. V. De Whalley, J. R. S. Hoult, J. Scott, and D. S. Leake. 1990. Alpha-tocopherol consumption during low density-lipoprotein oxidation. *Biochem. J.* **265:** 399–405.
5. Gebicki, J., G. Jürgens, and H. Esterbauer. 1992. Oxidation of low-density lipoprotein in vitro. *In* Oxidative Stress. H. Sies editor. Academic Press, London and San Diego. 371–397.
6. Esterbauer, H., G. Striegl, H. Puhl, and M. Dieber-Rotheneder. 1989. Continuous monitoring of in vitro oxidation of human low density lipoprotein. *Free Radical Res. Commun.* **6:** 67–75.
7. Gieseg, S. P., and H. Esterbauer. 1994. Low density lipoprotein is saturable by prooxidant copper. *FEBS Lett.* **343:** 188–194.
8. Puhl, H., G. Waeg, and H. Esterbauer. 1994. Methods to determine oxidation of low-density lipoproteins. *Methods Enzymol.* **233:** 425–441.
9. Kleinveld, H. A., H. L. M. Hak-Lemmers, A. F. H. Stalenhoef, and P. N. M. Demacker. 1992. Improved measurement of low-density-lipoprotein susceptibility to copper-induced oxidation: application of a short procedure for isolating low-density-lipoprotein. *Clin. Chem.* **38:** 2066–2072.
10. Schuster, B., R. Prassl, F. Nigon, M. J. Chapman, and P. Laggner. 1995. Core lipid structure is a major determinant of the oxidative resistance of low density lipoprotein. *Proc. Natl. Acad. Sci. USA.* **92:** 2509–2513.
11. Deckelbaum, R. J., G. G. Shipley, and D. M. Small. 1977. Structure and interactions of lipids in human plasma low density lipoproteins. *J. Biol. Chem.* **252:** 744–754.
12. Kostner, G. M., and P. Laggner. 1989. Chemical and physical properties of lipoproteins. *In* Human Plasma Lipoproteins. Clinical Biochemistry, Principles, Methods, Applications. J. C. Fruchart and J. Shepard, editors. Walter de Gruyter and Co., Berlin, New York. 23–54.
13. Herak, J. N., G. Pifat, J. Brnjas-Kraljevic, G. Lipka, K. Müller, and G. Knipping. 1988. Causal relationship between the transitions in the core and the surface in porcine low-density lipoproteins. *Chem. Phys. Lipids.* **48:** 135–139.
14. Berlin, E., and E. Sainz. 1984. Fluorescence polarization order parameters and phase transitions in lipids and lipoproteins. *Biochim. Biophys. Acta.* **794:** 49–55.
15. Walsh, M. T., and D. Atkinson. 1990. Calorimetric and spectroscopic investigation of the unfolding of human apolipoprotein B. *J. Lipid Res.* **31:** 1051–1062.
16. Walsh, M. T., and D. Atkinson. 1986. Physical properties of apoprotein B in mixed micelles with sodium deoxycholate and in a vesicle with dimyristoyl phosphatidylcholine. *J. Lipid Res.* **27:** 316–325.
17. Lehman, S., and H. L. Martin. 1982. Improved direct determination of alpha- and gamma-tocopherols in plasma and platelets by liquid chromatography, with fluorescence detection. *Clin. Chem.* **28:** 1784–1787.
18. Esterbauer, H., G. Jürgens, O. Quehenberger, and E. Koller. 1987. Autoxidation of human low density lipoprotein: loss of polyunsaturated fatty acids and vitamin E and generation of aldehydes. *J. Lipid Res.* **28:** 495–509.
19. Privalov, P. L., and S. A. Potehkin. 1986. Scanning microcalorimetry in studying temperature-induced changes in proteins. *Methods Enzymol.* **131:** 4–51.
20. Esterbauer, H., and G. Jürgens. 1993. Mechanistic and genetic aspects of susceptibility of LDL to oxidation. *Curr. Opin. Lipidol.* **4:** 114–124.
21. Spragg, S. P., and R. W. Wijnaendts van Resandt. 1984. The temperature dependence of the fluorescence decay of low-density lipoproteins. *Biochim. Biophys. Acta.* **792:** 84–91.
22. Herak, J. N. 1993. Physical changes of low-density lipoprotein on oxidation. *Chem. Phys. Lipids.* **66:** 231–234.
23. Lenaz, G., and M. Degli Esposti. 1994. Membrane bound enzymes. *In* Biomembrane: Structural and Functional Aspects. M. Shinitzky, editor. Balaban Publishers, Weinheim, New York, Basel, Cambridge, Tokyo, VCH. 164–177.
24. Esterbauer, H., M. Dieber-Rotheneder, G. Waeg, G. Striegl, and G. Jürgens. 1990. Biochemical, structural and functional properties of oxidized low-density lipoprotein. *Chem. Res. Toxicol.* **3:** 77–92.
25. Giessauf, A., E. Steiner, and H. Esterbauer. 1995. Early destruction of tryptophan residues of apolipoprotein B is a vitamin E independent process during copper-mediated oxidation of LDL. *Biochim. Biophys. Acta.* **1256:** 221–232.
26. Kveder, M., G. Pifat, S. Pe;abcar, and M. Schara. 1994. The ESR characterization of molecular mobility in the lipid surface layer of human serum lipoproteins. *Chem. Phys. Lipids.* **70:** 101–108.